

A Catalyst-Controlled Enantiodivergent Bromolactonization

Yuk-Cheung Chan,[†] Xinyan Wang,[†] Ying-Pong Lam, Jonathan Wong, Ying-Lung Steve Tse,^{*} and Ying-Yeung Yeung^{*}

Cite This: <https://doi.org/10.1021/jacs.1c05680>

Read Online

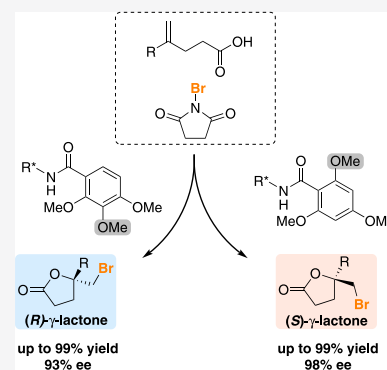
ACCESS |

Metrics & More

Article Recommendations

Supporting Information

ABSTRACT: A catalyst-controlled enantiodivergent bromolactonization of olefinic acids has been developed. Quinine-derived amino-amides bearing the same chiral core but different achiral aryl substituents were used as the catalysts. Switching the methoxy substituent in the aryl amide system from *meta*- to *ortho*-position results in a complete switch in asymmetric induction to afford the desired lactone in good enantioselectivity and yield. Mechanistic studies, including chemical experiments and density functional theory calculations, reveal that the differences in steric and electronic effects of the catalyst substituent alter the reaction mechanism.



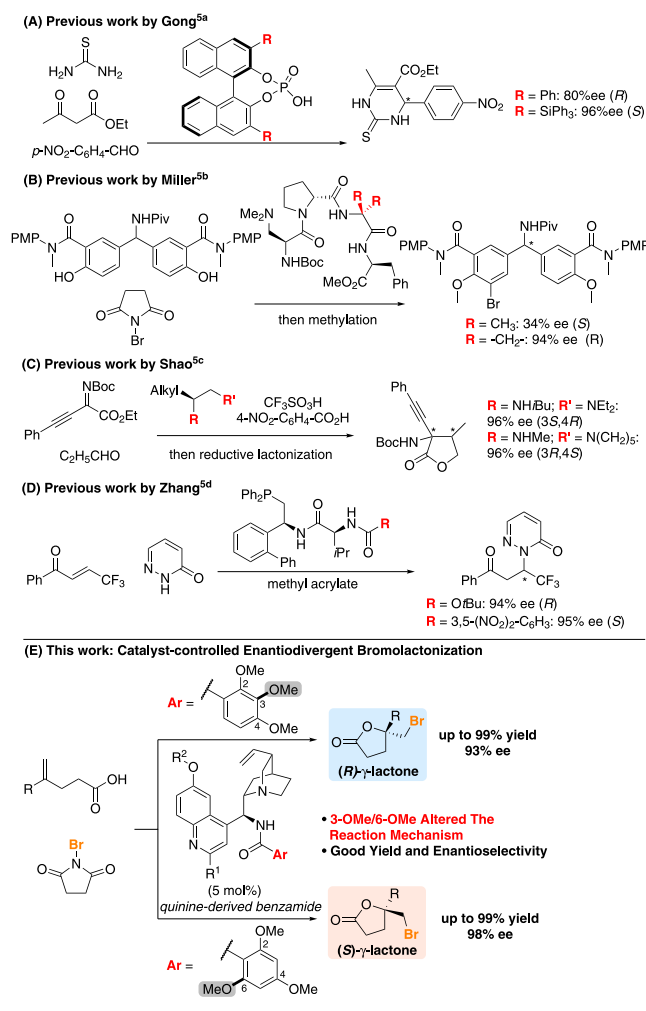
INTRODUCTION

Asymmetric catalysis is one of the most popular approaches for the preparation of enantioenriched compounds, which are of paramount importance in the synthesis of pharmaceuticals and natural products.¹ For comprehensive biological studies, it is highly desirable to have both antipodes of enantioenriched bioactive compounds.² However, it is not trivial to synthesize both hands of enantiomeric products in high optical purity in some circumstances because the exact antipodes of chiral catalyst scaffolds are not always available. A representative example is cinchona alkaloid-derived catalysts in which unnatural enantiomers of cinchona alkaloids are not readily available and their pseudoenantiomeric variants are not useful for comparison in many circumstances (see also Table S1 in SI).³ An appealing solution is enantiodivergent catalysis that enables the access to both antipodes of chiral products by utilizing catalysts with the same stereogenic element in the structural architecture. Different factors⁴ such as metal cations, reagents, ligand substituent, additives, anions, solvent and reaction time were identified to be tunable parameters in enantiodivergent asymmetric catalysis. Catalyst-controlled enantiodivergency, which involves the variation of the achiral residues remote from the chiral environment while keeping the stereogenic components and functional groups unchanged, is also an attractive approach but their reports are sporadic. A seminal work by Gong et al. demonstrated an efficient enantiodivergent Biginelli condensation catalyzed by chiral phosphoric acid in which the change in the substituents at the 3,3'-positions in the BINOL backbone brought a reversal of enantioselectivity (Scheme 1A).^{5a} In 2017, Miller et al. reported a desymmetrizing aromatic bromination of bis(phenols) with enantiodivergence originating from the alteration of the gem-

dimethyl to the cyclopropane achiral residue in the tetrapeptide catalyst (Scheme 1B).^{5b} Recently, Shao et al. have described a catalyst-controlled Mannich reaction by engineering the achiral residue of 1,2-diamine catalysts (Scheme 1C).^{5c} Zhang et al. reported enantiodivergent Michael addition controlled by dipeptide phosphines with achiral amide substituents in different solvents (Scheme 1D).^{5d} A highly relevant work was reported by Zhou et al. in which catalysts with different hydrogen-bond donors were used to create distinct chiral pockets for diastereodivergent Michael addition reactions.^{5e} Among the literature precedent of catalyst-controlled enantiodivergent catalysis, modifications of the steric and electronic properties at the achiral residues are the common strategies. However, to the best of our knowledge, utilization of regioisomeric catalyst to derive both antipodes of product efficiently remains unknown. Research on this direction could also provide a new pathway for catalyst design. Herein, we report the first case of catalyst-controlled enantiodivergent bromolactonization using a pair of quinine-derived regioisomeric catalysts (Scheme 1E). Quinine-derived benzamides were used as the chiral catalysts and altering the achiral methoxy substituents at the benzamides (i.e., regioisomers that have equal molecular weight) led to a switch in the enantioselectivity at synthetically useful level with a broad substrate scope.

Received: June 2, 2021

Scheme 1. Examples of Catalyst-Controlled Enantiodivergent Organocatalysis



Mechanistic studies were also undertaken to shed light on the origin of enantiodivergence and stereoinduction.

RESULTS AND DISCUSSION

Catalyst Study. Catalytic asymmetric halolactonization is an important approach to access chiral lactones, which are useful building blocks for medicinal chemistry and natural product synthesis. In addition, the resultant halogen handles in the lactone products can easily be manipulated to give various useful derivatives. Over the past few years, a number of research teams (including ours) have been devoted to this area and a number of catalytic systems have been developed.⁶ During our research endeavors,⁷ we identified that 9-*epi*-aminoquinine-derived catalyst **A0** that contains a benzamide achiral substituent could catalyze asymmetric bromolactonization of **1a** to (*R*)-**2a** using *N*-bromosuccinimide (NBS) with a promising enantioselectivity (27% ee) (Scheme 2). The enantioselectivity was improved when the catalyst bearing an electron-donating 2,4-dimethoxy substituent (i.e., **A1**) was used, giving (*R*)-**2a** in 65% ee. Unexpectedly, a reversed enantiomeric induction [78% ee of (*S*)-**2a**] was observed with the 2,6-dimethoxyphenyl catalyst **B1**. Further survey led us to identify that the 2,3,4-trimethoxyphenyl catalyst **A2** gave (*R*)-**2a** in 84% ee while the 2,4,6-trimethoxyphenyl catalyst **B2** gave the antipode (*S*)-**2a** in 82% ee. It is an unusual phenomenon because comparing catalyst

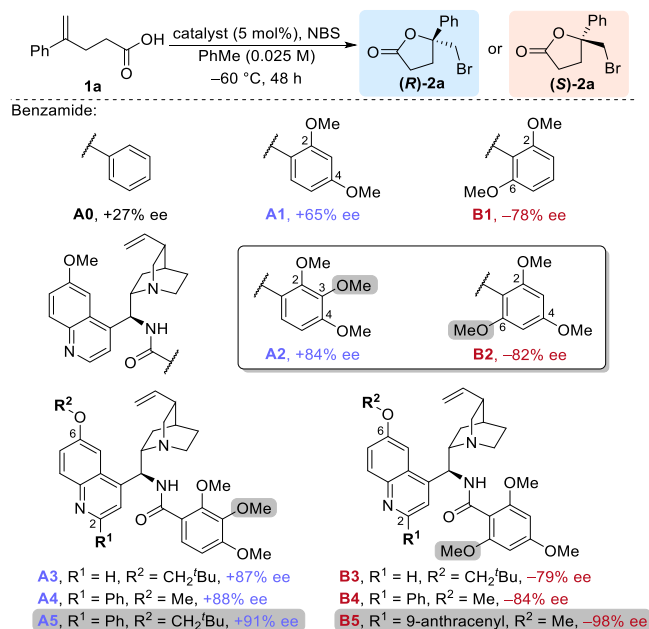
regioisomers **A2** and **B2** that have equal molecular weight, the only difference is the position of -OMe group (C3 or C6) that is several atoms away from the stereogenic element of the cinchona alkaloid skeleton. However, their asymmetric induction behavior is notably different.

Encouraged by this interesting result, we further investigated catalysts with other substituents in the quinoline system⁸ and a steric-matching preference between the benzamide and the quinoline moiety was observed (Scheme 2). For instance, the 2,3,4-trimethoxyphenyl (2,3,4-OMe) catalyst system favors a bulky substituent at C(6) with concomitant medium-sized phenyl group at C(2) on quinoline, making **A5** an optimized catalyst (for the rest of combinations, see Table S2 in SI). However, the 2,4,6-trimethoxyphenyl (2,4,6-OMe) catalyst system showed an opposite trend. Raising the steric hindrance from Me to *neo*-pentyl at C(6) of quinoline gave a disappointing result; meanwhile, a very bulky 9-anthracenyl at C(2) significantly improved the enantiomeric induction to give **B5** as another lead catalyst. This matching preference between 2,3,4-OMe/2,4,6-OMe and quinoline residues suggests the catalysts adopt a different pocket for substrate binding and might eventually contribute to the enantiodivergence.

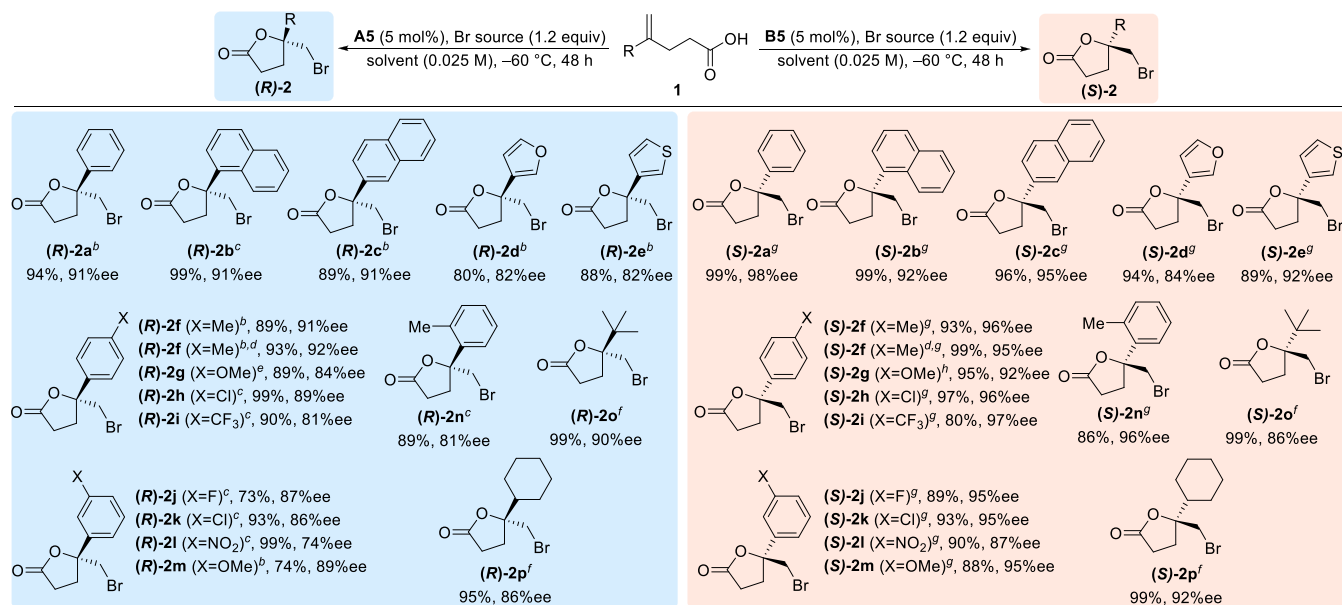
Substrate Scope. With the optimized catalysts (**A5** and **B5**) and reaction conditions (for a brief optimization of solvent and bromine source, see Tables S1 and S3 in SI) in hand, the scope of bromolactonization of **1** was evaluated and the results are summarized in Scheme 3.

- Scope of 1,1-disubstituted olefinic acids by catalyst **A5**: Lactonization of both electron-neutral and donating substituents of aryl olefinic acids **1**, including heterocycles (**1d**, **1e**), were catalyzed smoothly to give (*R*)-**2** in good yield and enantioselectivity catalyzed by the 2,3,4-OMe catalyst **A5**. For substrates bearing electron-withdrawing groups, e.g., halogen, CF₃, and NO₂, a stronger brominating agent *N,N*-dibromohydantoin (DBDMH) was needed for good conversion.
- Scope of 1,1-disubstituted olefinic acids by catalyst **B5**: The 2,4,6-OMe catalyst **B5** also efficiently promoted the bromolactonization for a wide range of substrates **1** to give (*S*)-**2** in good yield and enantioselectivity using either NBS or DBDMH as the brominating source. The catalytic performance is comparable to that of **A5**. The asymmetric induction was also found to be less influenced by the electronic and steric properties of the substrates. Interestingly, our new catalyst of amino-benzamide works well with substrate bearing *para*-OMe (**1g**) and *ortho*-Me (**1n**) substituent, which were either less selective or reactive in previous bromolactonization studies.^{7,9} Within the scope, no substrate-controlled enantiomeric switch was observed.¹⁰
- Scope of 1,2-disubstituted olefinic acids: We also extended the scope to 1,2-disubstituted olefinic substrates that gave rise to products with two stereogenic centers (Scheme 4). It was found that the enantiodivergent methodology could be applied to 1,2-*trans*- and 1,2-*cis*-disubstituted olefinic acids **1q** and **1r**, giving both antipodes of **2q** and **2r**, respectively, in good yield and enantioselectivity. The excellent *endo* (for **2q**) and *exo* (for **2r**) selectivity could be attributed to the steric and electronic effects of the *trans*- and *cis*-olefins.^{6j}

Structural Analysis of the Catalysts. Several studies were conducted in order to get a better understanding on the

Scheme 2. Effect of the Catalyst Substituents^a

^aReactions were carried out at 0.05 mmol scale under N_2 in the absence of light. All conversions were determined to be >95% using ^1H NMR. Enantiomeric excess (ee) was determined by HPLC on a chiral stationary phase. Positive and negative signs of ee are assigned for **(R)-2a** and **(S)-2a**, respectively.

Scheme 3. Substrate Scope of the Enantiodivergent Bromolactonization of 1,1-Substituted Olefinic Acids^a

^aReactions were carried out on 0.1 mmol scale under N_2 in the absence of light. Enantiomeric excess (ee) was determined by HPLC on a chiral stationary phase. ^bNBS, PhMe/*m*-xylene (2:1 v/v). ^cDBDMH, PhMe/PhCl (4:1 v/v). ^dOne mmol scale, 96 h. ^eDBDMH, PhMe/*o*-xylene (2:1 v/v). ^fDBDMH, PhMe. ^gNBS, PhMe/*o*-xylene (2:1 v/v). ^hNBS, PhMe/ CHCl_3 (4:1 v/v).

structural differences between the two catalyst regioisomers. We speculate that the difference associated with the amide group (both sterically and electronically) of the catalysts might play a crucial role in dictating the mechanistic pathway. Since cinchona alkaloids derivatives are known to exist in several conformers,¹¹ the population of conformers might be expected to affect the enantioselectivity.¹² Thus, we analyzed the structural difference between catalysts **A2** and **B2**. For catalyst **A2**, strong nuclear Overhauser effect (NOE) correlations were observed between

$\text{H}^1\text{-H}^9$ and $\text{H}^5\text{-H}^8$, suggesting that **A2** exhibited *anti*-open-1 conformation in majority (Figure 1A). Meanwhile, strong NOE correlations were observed in $\text{H}^1\text{-H}^9$, $\text{H}^5\text{-H}^8$, and $\text{H}^5\text{-H}^{11}$ in the case of **B2**, indicating that it might also adopt an *anti*-open-2 conformation. While both **A2** and **B2** adopted “open” conformations which were consistent with the conformational analysis of 9-*epi*-quinine,¹³ the slight difference (based on the NOE correlations) in the catalyst geometry could be attributed to the difference in the steric demand between the 2,3,4- and

Scheme 4. Asymmetric Bromolactonization of 1,2-Disubstituted Olefinic Acids

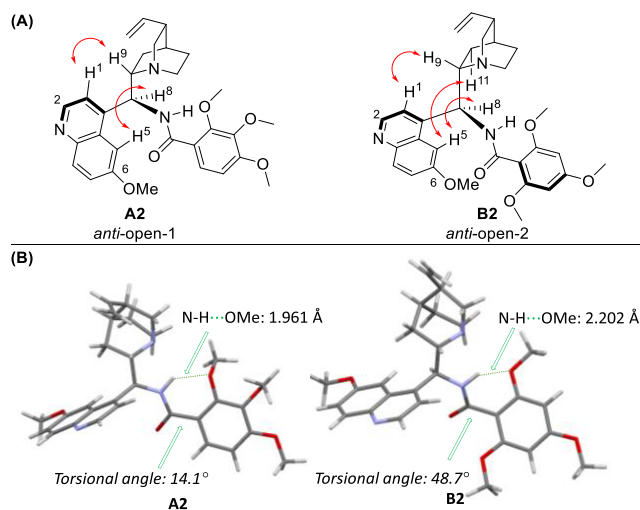
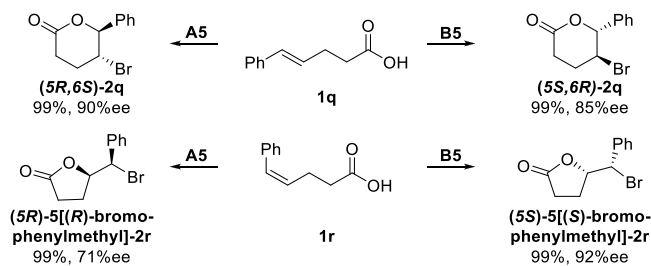
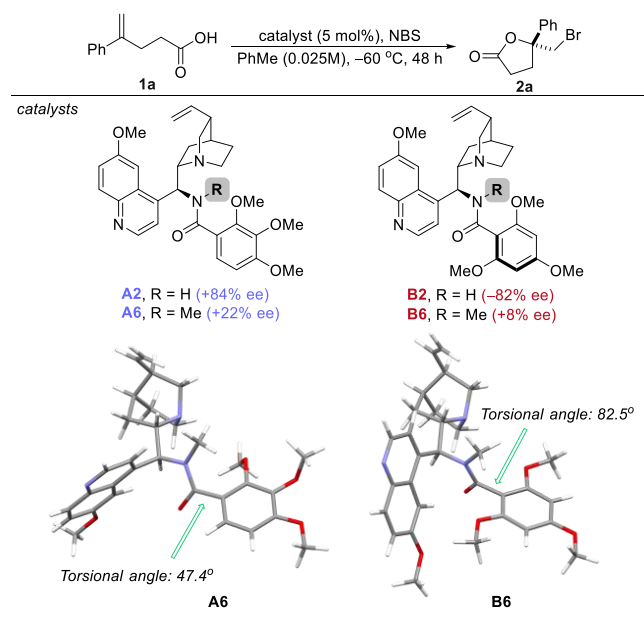


Figure 1. Structural analysis. (A) NOE study of catalysts **A2** and **B2**. (B) Optimized structures of **A2** and **B2** by DFT.

2,4,6-trimethoxyphenyl substituents, consistent with the optimized structures of **A2** and **B2** by density functional theory (DFT) at the level of M06-2X-D3/6-311G(d,p) (Figure 1B; also see Figures S2–S3 in SI). The calculated torsion angles between the amide and phenyl planes in **A2** is 14.1°, which is comparable to the measured value (15.5°) from X-ray crystallography of **A2** single crystal. The calculated torsion angle in **B2** (>48.7°) is much larger, attributed to the steric hindrance of the two methoxy groups at the *ortho*-position (also see Figure S1 in SI). Another key structural difference between two catalysts is the close contact between N–H...OMe (1.961 Å) in **A2**. This suggested the N–H in **A2** interacts with *ortho*-OMe in the benzamide via intramolecular hydrogen bond. The weak intramolecular H-bond in **B2** (indicated by the relatively longer N–H...OMe 2.20–2.90 Å) could be attributed to the heavily distorted benzamide geometry. We then speculated the presence of intramolecular hydrogen bond might be a crucial factor behind the enantiodivergence since no distinct difference in conformation of catalyst was observed.

Role of N–H in the Benzamide Catalysts. We prepared and evaluated the catalytic performance of methylated benzamide **A6** and **B6** as analogues of **A2** and **B2**, respectively (Scheme 5). Albeit the enantioselectivity dropped dramatically for both N–Me catalysts **A6** and **B6**, presumably due to the involvement of hydrogen bond from amide's N–H in the stereodetermining step. Moreover, the reversal of asymmetric induction completely disappeared in **B6**, further highlighting the crucial role of free N–H amide. On the basis of the DFT calculation, the torsion angles at the N–Me aryl moieties of **A6**

Scheme 5. Comparison of the N–H and N–Me Benzamide Catalysts



and **B6** are 47.4° and 82.5°, respectively. These values are considerably higher than that of the N–H catalysts **A2** and **B2**, attributed to the loss of hydrogen bond and increase in steric effect. In combination with the results from the structural analysis of the N–H catalysts (Figure 1), we hypothesize the origin of enantiodivergence might come from a different binding model or sequence between catalyst and substrate or reagent (Br source), which could be strongly influenced by the presence of a free N–H amide. Indeed, recent studies by Borhan et al. nicely demonstrated that fragment interaction among halogen source, catalyst, and olefinic acid is crucial for highly enantioselective chlorolactonization.¹⁴

Theoretical Study. Density functional theory (DFT) calculations were carried out in order to elucidate the origin of the distinct difference in asymmetric performance of the two catalysts. The geometry optimizations and single-point energies were carried out using Gaussian 09 (ver. D.01) at the levels of M06-2X-D3/6-311G(d) and M06-2X-D3/6-311++G(d,p), respectively.¹⁵ The SMD solvent model¹⁶ was used. All the thermodynamic properties were evaluated at 213 K.

a. Free Energy Profile with Catalyst A2. We found in the calculated free energy profile with catalyst **A2** that the quinuclidine's nitrogen in catalyst **A2** coordinates with the Br of NBS while the amide N–H hydrogen bonds with the *ortho*-methoxy in the aryl substituent (Figure 2). Concurrently, the carboxylic acid substrate protonates the succinimide's carbonyl oxygen to give the trilateral complex **R1**. Subsequently, the succinimide dissociates from Br via **TS1** with a free energy barrier of 17.4 kcal mol⁻¹ to give intermediates **IM1**. A conformational change together with the formation of a hydrogen bond between succinimide oxygen and the N–H in catalyst's amide moiety give **IM2**. Then, formation of the bromiranium intermediate **IM3a** proceeds via **TS2a**. Finally, cyclization of **IM3a** via **TS3a** gives the major product (*R*)-**2a**. The rate-determining step is **R1** → **TS1** while the enantiodetermining step is **IM2** → **TS3a**. For the pathway toward the minor product (*S*)-**2a**, the barrier of the enantiodetermining step from **IM2** to **TS2b** (6.3 kcal mol⁻¹) is significantly higher than that in the major pathway from **IM2**

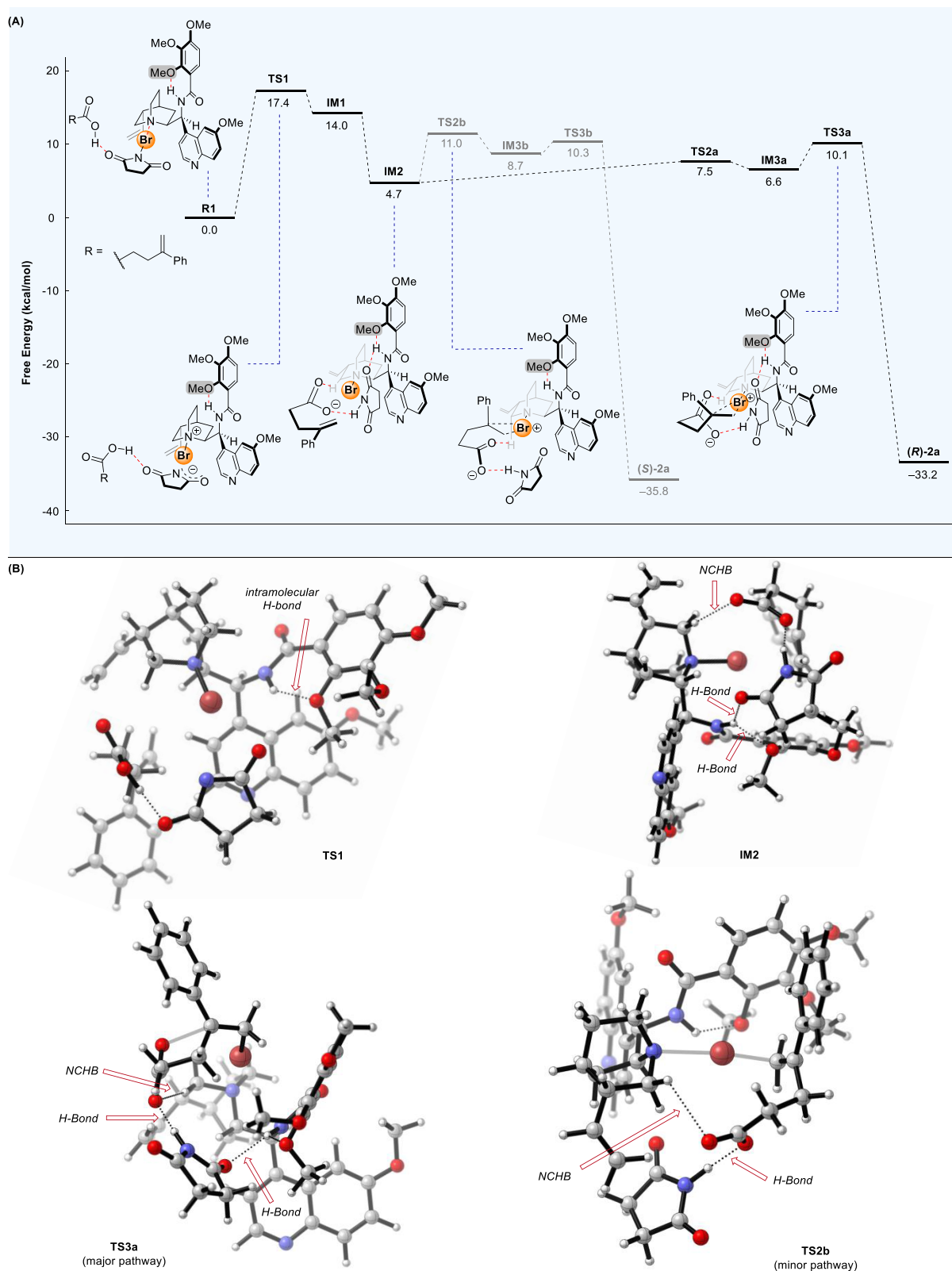


Figure 2. Free energy profile of the A2-catalyzed reaction.

to TS3a ($5.4 \text{ kcal mol}^{-1}$). Throughout the free energy profile, it was observed that the intramolecular hydrogen bond persists. As compared with TS3a, the hydrogen bond between the succinimide oxygen and the N–H of catalyst's amide group is missing in TS2b. In addition, it was found that the α -C–H of the

ammonium cation moiety stabilizes the carbonyl group of the substrate in the major pathway more significantly (*vide infra*), which could justify the lower free energy of TS3a versus TS2b.

b. Free Energy Profile of System with Catalyst B2. For catalyst B2, the initial stage R2 involves the complexation of the

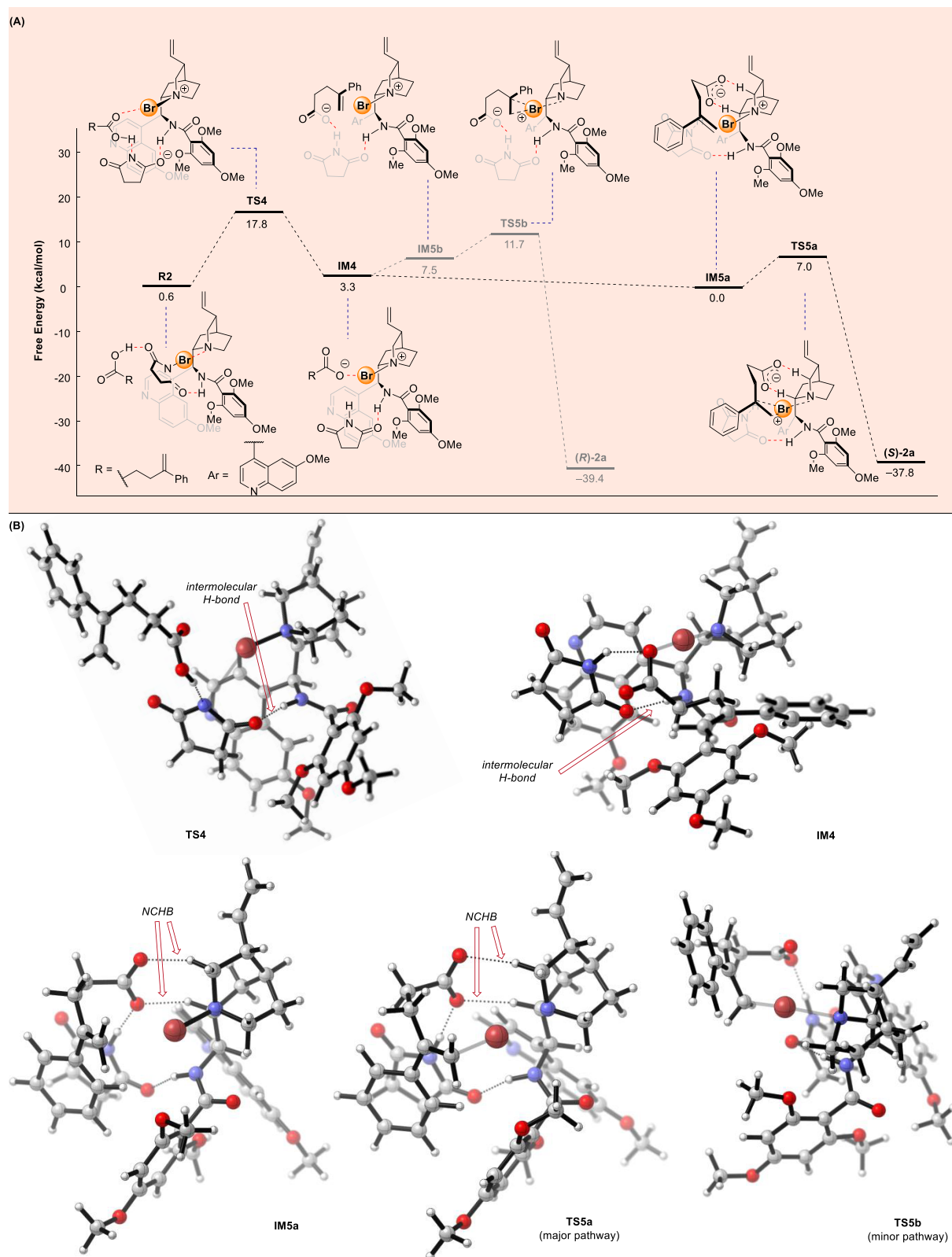


Figure 3. Free energy profile of the B2-catalyzed reaction.

catalyst and NBS via the following: (1) N–Br interaction between quinuclidine’s nitrogen and NBS; (2) hydrogen bond interaction between the amide N–H and the succinimide carbonyl oxygen (Figure 3). This result is consistent with the structural analysis in which the large torsion angle between the

amide and the aryl moieties restricts the formation of intramolecular hydrogen bond (Figure 1). The Br is transferred from succinimide to the quinuclidine. Concurrently, protonation of succinimide gives the carboxylate that interacts with the Br. The whole process ($R2 \rightarrow IM4$ via $TS4$) has a free energy

barrier of 17.2 kcal mol⁻¹, which is the rate-determining step. Next, conformational change of **IM4** followed by bromination gives the bromiranium intermediate **IM5a**. Cyclization of **IM5a** via **TSSa** furnishes (*S*)-**2a** as the major product. The enantiodetermining step in the major product formation is the step from **IM5a** to **TSSa** (barrier = 7.0 kcal mol⁻¹), whose rate is significantly faster than that of the minor pathway from **IM4** to **TSSb** (barrier = 8.4 kcal mol⁻¹). **TSSa** is substantially stabilized as compared with **TSSb** for reasons explained in the next section.

There is a major difference when comparing the two catalytic systems. In catalyst **A2**, the intramolecular hydrogen bond restrains the geometry of the aryl amide. Thus, the 2,3,4-trimethoxy benzamide appears to mainly serve as a steric shield group in the reaction. For catalyst **B2**, however, the amide's N–H is available to interact with NBS throughout the process. The enantioselectivity is likely to be controlled by both functionalities (quinuclidine and amide) in the catalyst. This key factor might govern the enantiodivergent bromolactonization.

c. Stabilization Effect in the Reactions. To get a better understanding of the enantiodetermining steps in **Figures 2** and **3**, Natural Bond Orbital (NBO)¹⁷ and Atoms In Molecules (AIM)¹⁸ analyses were carried out to understand the interactions. For **TS3a** of the **A2**-catalyzed reaction, the NBO charge of the α -C–H of the ammonium cation (+0.23 as shown in **Figure 4A** inset) is markedly more positive than those of the typical C–H's (about +0.20) because of the electropositivity of the ammonium nitrogen. In addition, the NBO charge of the carboxylate oxygen is calculated to be –0.82. The relatively

larger difference in the NBO charges between the C–H and C–O along with the short interatomic distances (2.5 Å), the α -C–H interacts strongly with the carboxylate oxygen and form what can be classified as a nonclassical hydrogen bond (NCHB)¹⁹ as indicated by the bond path and critical point (green and orange) from AIM.²⁰ Such a bond path indicates where the electron density is maximally concentrated between the two nuclei and shows the directionality of an interaction. The corresponding NCHB in **TS2b** of the minor pathway is considerably weaker (see **SI** for detail), and we believe this difference is one of the major factors for the lower free energy of **TS3a** than that of **TS2b** by about 0.9 kcal mol⁻¹, leading to the enantioselectivity.

Similarly, there are NCHBs in **TSSa** of the **B2**-catalyzed reaction. By also carrying out an AIM analysis, we determined the bond paths and critical points²⁰ that indicate the directions and paths of maximal electron density of the significant intermolecular interactions, which include the π – π interaction in addition to NCHBs in **Figure 4B**. There are no such NCHBs and π – π interaction in **TSSb** of the minor pathway (**Figure 3B**), which can explain why **TSSa** has a lower free energy than **TSSb** by 4.7 kcal mol⁻¹. This free energy difference is larger than that of the enantiodetermining step in the **A2**-catalyzed reaction, plausibly due to the fact that both the NCHBs and π – π interaction are at play.²¹

Electronic Effect of the Substituents. Since the *ortho*-oxygen was found to be crucial for the high enantioselectivity with the 2,3,4-trimethoxy catalyst **A5** (or **A2**), it is expected that the electronic property of the aryl group would affect the asymmetric performance. On the basis of our calculations on the catalyst structure (**Figure 1**), it appears that the hydrogen bond between the N–H and the *ortho*-oxygen in the aryl group might be crucial for the high enantioselectivity. A more detailed study was conducted by varying the R substituents including methoxy, methoxymethoxy (OMOM), difluoromethoxy, and triflate (OTf) at the *para*-position of the phenyl ring (i.e., catalysts **A7**–**A10**). A slight modification of the catalyst (using 2,3-methylenedioxy instead of 2,3-dimethoxy) was undertaken to minimize the steric effect brought by the substituents.²² It is interesting to observe that a higher ee of product (*R*)-**2a** could be obtained with a more electron-donating substituent at the *para*-position (**Figure 5**). In addition, the $\Delta\Delta G^\ddagger$ and Hammett σ_{para} coefficient²³ could be correlated in which a negative slope of plot was observed.²⁴ The Hirshfeld atomic charge of the *ortho*-oxygen (O_A) was calculated and its negative charge was found to become more positive with the increasing electron-donating ability of the R substituent at the *para*-position and higher enantioselectivity in general. This is consistent with the result that the *ortho*-oxygen interacts with the amide via hydrogen bond and such interaction might restrain the geometry of the catalyst that is crucial for high ee.

CONCLUSION

In summary, we have developed a catalyst-controlled enantiodivergent bromolactonization with both (*R*)- and (*S*)-products in good yield and optical purity. Mechanistic studies suggest that the amides in the 2,3,4-trimethoxyphenyl catalyst **A5** and the 2,4,6-trimethoxyphenyl catalyst **B5** might serve different functions, leading to the enantiodivergent behavior. This study provides an alternative approach toward asymmetric halocyclization through catalyst substituent manipulation. This study also highlights that achiral substituents on chiral catalysts may serve not only in steric-shielding but also in switching reaction mechanisms.

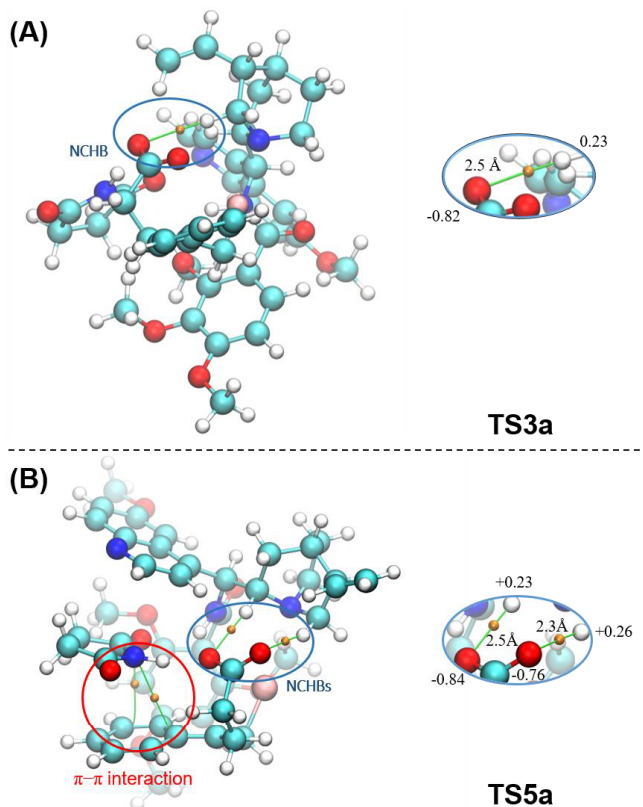


Figure 4. (A) Optimized structure of **TS3a**. (B) Optimized structure of **TS5a**. Bond paths and critical points computed by an AIM analysis (green lines and orange dots) show both the nonclassical hydrogen bonds (NCHBs) and π – π interaction. NBO charges and NCHB distances of the atoms involved are shown in the insets.

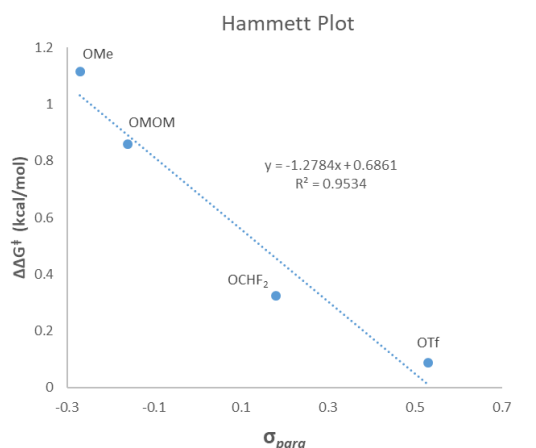
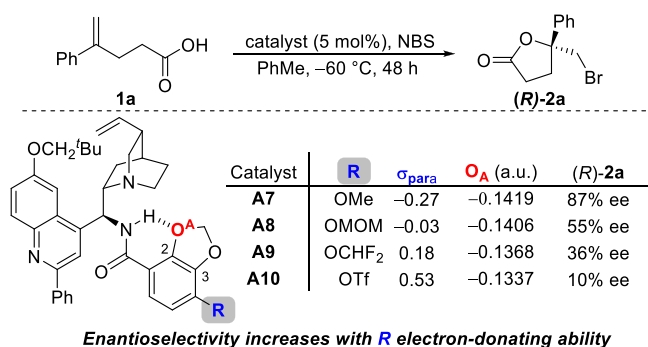


Figure 5. Relationship between enantioselectivity and σ_{para} of R.

ASSOCIATED CONTENT

Supporting Information

The Supporting Information is available free of charge at <https://pubs.acs.org/doi/10.1021/jacs.1c05680>.

Experimental procedure, NMR spectra, characterization data, computational data (PDF)

Accession Codes

CCDC 2087453–2087455 contain the supplementary crystallographic data for this paper. These data can be obtained free of charge via www.ccdc.cam.ac.uk/data_request/cif, or by emailing data_request@ccdc.cam.ac.uk, or by contacting The Cambridge Crystallographic Data Centre, 12 Union Road, Cambridge CB2 1EZ, UK; fax: +44 1223 336033.

AUTHOR INFORMATION

Corresponding Authors

Ying-Lung Steve Tse – Department of Chemistry and State Key Laboratory of Synthetic Chemistry, The Chinese University of Hong Kong, Hong Kong, China; orcid.org/0000-0003-1187-2296; Email: stevetse@cuhk.edu.hk

Ying-Yeung Yeung – Department of Chemistry and State Key Laboratory of Synthetic Chemistry, The Chinese University of Hong Kong, Hong Kong, China; orcid.org/0000-0001-9881-5758; Email: yyeung@cuhk.edu.hk

Authors

Yuk-Cheung Chan – Department of Chemistry and State Key Laboratory of Synthetic Chemistry, The Chinese University of Hong Kong, Hong Kong, China

Xinyan Wang – Department of Chemistry and State Key Laboratory of Synthetic Chemistry, The Chinese University of

Hong Kong, Hong Kong, China; orcid.org/0000-0002-3690-2335

Ying-Pong Lam – Department of Chemistry and State Key Laboratory of Synthetic Chemistry, The Chinese University of Hong Kong, Hong Kong, China

Jonathan Wong – Department of Chemistry and State Key Laboratory of Synthetic Chemistry, The Chinese University of Hong Kong, Hong Kong, China; orcid.org/0000-0002-1187-063X

Complete contact information is available at: <https://pubs.acs.org/10.1021/jacs.1c05680>

Author Contributions

[†]Y.C.C. and X.W. contributed equally.

Notes

The authors declare no competing financial interest.

ACKNOWLEDGMENTS

We thank the HKSAR University Grant Council (Grant No. CUHK 14305520) and The Chinese University of Hong Kong Direct Grant (Grant No. 4053275, 4053329, 4053203, 4053449), and Innovation and Technology Commission to the State Key Laboratory of Synthetic Chemistry (GHP/004/16GD) for financial support. This paper is dedicated to Professor Henry N. C. Wong on the occasion of his 70th Birthday.

REFERENCES

- (1) (a) Liu, G.-Q.; Li, Y.-M.; Chan, A. S. C. *Principles and Applications of Asymmetric Synthesis*; John Wiley & Sons, Inc: New York, 2001; pp 1–69. (b) Blaser, H. U. The Chiral Pool as a Source of Enantioselective Catalysts and Auxiliaries. *Chem. Rev.* **1992**, *92*, 935–952.
- (2) (a) Abraham, D. J.; Rotella, D. P. *Burger's Medicinal Chemistry, Drug Discovery, and Development*, 7th ed.; John Wiley & Sons, Inc: New York, 2010; pp 127–166. (b) Nguyen, L. A.; He, H.; Pham-Huy, C. Chiral Drugs: An Overview. *Int. J. Biomed. Sci.* **2006**, *2*, 85–100.
- (3) Hu, B.; Bezpalko, M. W.; Fei, C.; Dickie, D. A.; Foxman, B. M.; Deng, L. Origin of and a Solution for Uneven Efficiency by Cinchona Alkaloid-Derived, Pseudoenantiomeric Catalysts for Asymmetric Reactions. *J. Am. Chem. Soc.* **2018**, *140*, 13913–13920.
- (4) For selected reviews (and the references listed) and examples for enantiodivergent catalysis, see: (a) Zanoni, G.; Castronovo, F.; Franzini, M.; Vidari, G.; Giannini, E. Toggling Enantioselective Catalysis—A Promising Paradigm in the Development of More Efficient and Versatile Enantioselective Synthetic Methodologies. *Chem. Soc. Rev.* **2003**, *32*, 115–129. (b) Bartók, M. Unexpected Inversions in Asymmetric Reactions: Reactions with Chiral Metal Complexes, Chiral Organocatalysts, and Heterogeneous Chiral Catalysts. *Chem. Rev.* **2010**, *110*, 1663–1705. (c) Escorihuela, J.; Burguete, M. I.; Luis, S. V. New Advances in Dual Stereocontrol for Asymmetric Reactions. *Chem. Soc. Rev.* **2013**, *42*, 5595–5617. (d) Beletskaya, I. P.; Nájera, C.; Yus, M. Stereodivergent Catalysis. *Chem. Rev.* **2018**, *118*, 5080–5200. (e) Garzan, A.; Jaganathan, A.; Marzijarani, N. S.; Yousefi, K.; Whitehead, D. C.; Jackson, J. E.; Borhan, B. Solvent-Dependent Enantiodivergence in the Chlorocyclization of Unsaturated Carbamates. *Chem. - Eur. J.* **2013**, *19*, 9015–9021. (f) Neel, A. J.; Milo, A.; Sigman, M. S.; Toste, F. D. Enantiodivergent Fluorination of Allylic Alcohols: Data Set Design Reveals Structural Interplay between Achiral Directing Group and Chiral Anion. *J. Am. Chem. Soc.* **2016**, *138*, 3863–3875. (g) Jiang, H.-J.; Liu, K.; Yu, J.; Zhang, L.; Gong, L.-Z. Switchable Stereoselectivity in Bromoaminocyclization of Olefins: Using Brønsted Acids of Anionic Chiral Cobalt(III) Complexes. *Angew. Chem., Int. Ed.* **2017**, *56*, 11931–11935. (h) Hayama, N.; Kobayashi, Y.; Sekimoto, E.; Miyazaki, A.; Inamoto, K.; Kimachi, T.; Takemoto, Y. A Solvent-Dependent Chirality

Switchable Thia-Michael Addition to α,β -Unsaturated Carboxylic Acids Using a Chiral Multifunctional Thiourea Catalyst. *Chem. Sci.* **2020**, *11*, 5572–5576. (i) Tu, H.-F.; Yang, P.; Lin, Z.-H.; Zheng, C.; You, S.-L. Time-dependent enantiodivergent synthesis via sequential kinetic resolution. *Nat. Chem.* **2020**, *12*, 838–844.

(5) For selected examples of catalyst achiral residue controlling enantiomeric induction, see: (a) Li, N.; Chen, X.-H.; Song, J.; Luo, S.-W.; Fan, W.; Gong, L.-Z. Highly Enantioselective Organocatalytic Biginelli and Biginelli-Like Condensations: Reversal of the Stereochemistry by Tuning the 3,3'-Disubstituents of Phosphoric Acids. *J. Am. Chem. Soc.* **2009**, *131*, 15301–15310. (b) Hurtley, A. E.; Stone, E. A.; Metrano, A. J.; Miller, S. J. Desymmetrization of Diarylmethylamido Bis(phenols) through Peptide-Catalyzed Bromination: Enantiodivergence as a Consequence of a 2 amu Alteration at an Achiral Residue within the Catalyst. *J. Org. Chem.* **2017**, *82*, 11326–11336. (c) Dai, J.; Wang, Z.; Deng, Y.; Zhu, L.; Peng, F.; Lan, Y.; Shao, Z. Enantiodivergence by Minimal Modification of An Acyclic Chiral Secondary Aminocatalyst. *Nat. Commun.* **2019**, *10*, 5182. (d) Wang, H.; Li, X.; Tu, Y.; Zhang, J. Catalytic Enantiodivergent Michael Addition by Subtle Adjustment of Achiral Amino Moiety of Dipeptide Phosphines. *iScience* **2020**, *23*, 101138. (e) Ding, P.-G.; Zhou, F.; Wang, X.; Zhao, Q.-H.; Yu, J.-S.; Zhou, J. H-Bond Donor-Directed Switching of Diastereoselectivity in the Michael addition of α -Azido Ketones to Nitroolefins. *Chem. Sci.* **2020**, *11*, 3852–3861.

(6) For selected reviews (and the references cited therein) and examples on organocatalytic asymmetric chloro-/bromo-/iodo-lactonization, see: (a) Denmark, S. E.; Kuester, W. E.; Burk, M. T. Catalytic, Asymmetric Halofunctionalization of Alkenes—A Critical Perspective. *Angew. Chem., Int. Ed.* **2012**, *51*, 10938–10953. (b) Tan, C. K.; Yeung, Y.-Y. Recent Advances in Stereoselective Bromofunctionalization of Alkenes using N-bromoamide Reagents. *Chem. Commun.* **2013**, *49*, 7985–7996. (c) Zheng, S.; Schienebeck, C. M.; Zhang, W.; Wang, H.-Y.; Tang, W. Cinchona Alkaloids as Organocatalysts in Enantioselective Halofunctionalization of Alkenes and Alkynes. *Asian J. Org. Chem.* **2014**, *3*, 366–376. (d) Nolsøe, J. M. J.; Hansen, T. V. Asymmetric Iodolactonization: An Evolutionary Account. *Eur. J. Org. Chem.* **2014**, *2014*, 3051–3065. (e) Kristianslund, R.; Tungen, J. E.; Hansen, T. V. Catalytic Enantioselective Iodolactonization. *Org. Biomol. Chem.* **2019**, *17*, 3079–3092. (f) Mao, B.; Fañanas-Mastral, M.; Feringa, B. L. Catalytic Asymmetric Synthesis of Butenolides and Butyrolactones. *Chem. Rev.* **2017**, *117*, 10502–10566. (g) Han, X.; Dong, C.; Zhou, H.-B. C3-Symmetric Cinchonine-Squaramide-Catalyzed Asymmetric Chlorolactonization of Styrene-Type Carboxylic Acids with 1,3-Dichloro-5,5-dimethylhydantoin: An Efficient Method to Chiral Isochroman-1-one. *Adv. Synth. Catal.* **2014**, *356*, 1275–1280. (h) Knowe, M. T.; Danneman, M. W.; Sun, S.; Pink, M.; Johnston, J. N. Biomimetic Desymmetrization of a Carboxylic Acid. *J. Am. Chem. Soc.* **2018**, *140*, 1998–2001. (i) Arai, T.; Horigane, K.; Watanabe, O.; Kakino, O.; Sugiyama, N.; Makino, H.; Kamei, Y.; Yabe, S.; Yamanaka, M. Association of Halogen Bonding and Hydrogen Bonding in Metal Acetate-Catalyzed Asymmetric Halolactonization. *iScience* **2019**, *12*, 280–292. (j) Klosowski, D. W.; Hethcox, J. C.; Paull, D. H.; Fang, C.; Donald, J. R.; Shugrue, C. R.; Pansick, A. D.; Martin, S. F. Enantioselective Halolactonization Reactions using BINOL-Derived Bifunctional Catalysts: Methodology, Diversification, and Applications. *J. Org. Chem.* **2018**, *83*, 5954–5968. (k) Whitehead, D. C.; Yousefi, R.; Jaganathan, A.; Borhan, A. An Organocatalytic Asymmetric Chlorolactonization. *J. Am. Chem. Soc.* **2010**, *132*, 3298. (l) Veitch, G. E.; Jacobsen, E. N. Tertiary Aminourea-Catalyzed Enantioselective Iodolactonization. *Angew. Chem., Int. Ed.* **2010**, *49*, 7332–7335.

(7) (a) Zhou, L.; Tan, C. K.; Jiang, X.; Chen, F.; Yeung, Y.-Y. Asymmetric Bromolactonization Using Amino-Thiocarbamate Catalyst. *J. Am. Chem. Soc.* **2010**, *132*, 15474–15476. (b) Tan, C. K.; Zhou, L.; Yeung, Y.-Y. Aminothiocabamate-Catalyzed Asymmetric Bromolactonization of 1,2-Disubstituted Olefinic Acids. *Org. Lett.* **2011**, *13*, 2738–2741. (c) Tan, C. K.; Le, C.; Yeung, Y.-Y. Enantioselective Bromolactonization of Cis-1,2-disubstituted Olefinic Acids Using an Amino-Thiocarbamate Catalyst. *Chem. Commun.* **2012**, *48*, 5793–5795. (d) Chen, J.; Zhou, L.; Tan, C. K.; Yeung, Y.-Y. An

Enantioselective Approach toward 3,4-Dihydroisocoumarin through the Bromocyclization of Styrene-type Carboxylic Acids. *J. Org. Chem.* **2012**, *77*, 999–1099. (e) Jiang, X.; Tan, C. K.; Zhou, L.; Yeung, Y.-Y. Enantioselective Bromolactonization Using an S-Alkyl Thiocarbamate Catalyst. *Angew. Chem., Int. Ed.* **2012**, *51*, 7771–7775. (f) Zheng, T.; Wang, X.; Ng, W.-H.; Tse, Y.-L. S.; Yeung, Y.-Y. Catalytic Enantio- and Diastereoselective Domino Halocyclization and Spiroketalization. *Nature Catalysis* **2020**, *3*, 993–1001.

(8) (a) Lee, H.-J.; Cho, C.-W. Cinchona-Based Primary Amine-Catalyzed Asymmetric Cascade Aza-Michael–Aldol Reactions of Enones with 2-(1H-Pyrrol-2-yl)-2-oxoacetates: Synthesis of Chiral Pyrrolizines with Multistereocenters. *J. Org. Chem.* **2013**, *78*, 3306–3312. (b) Jurberg, I. D. An Aminocatalyzed Stereoselective Strategy for the Formal α -Propargylation of Ketones. *Chem. - Eur. J.* **2017**, *23*, 9716–9720.

(9) (a) Nishikawa, Y.; Hamamoto, Y.; Satoh, R.; Akada, N.; Kajita, S.; Nomoto, M.; Miyata, M.; Nakamura, M.; Matsubara, C.; Hara, O. Enantioselective Bromolactonization of Trisubstituted Olefinic Acids Catalyzed by Chiral Pyridyl Phosphoramides. *Chem. - Eur. J.* **2018**, *24*, 18880–18885. (b) Kristianslund, R.; Hansen, T. V. Enantioselective Bromolactonization of Aryl Functionalized Alkenoic Acids. *Tetrahedron Lett.* **2020**, *61*, 151756.

(10) For selected examples for substrate controlled enantiodivergency, see: (a) Corrêa, R. J.; Garden, S. J.; Angelici, G.; Tomasini, C. A DFT and AIM Study of the Proline-Catalyzed Asymmetric Cross-Aldol Addition of Acetone to Isatins: A Rationalization for the Reversal of Chirality. *Eur. J. Org. Chem.* **2008**, *2008*, 736–744. (b) Featherston, A. L.; Shugrue, C. R.; Mercado, B.; Miller, S. J. Phosphothreonine (pThr)-Based Multifunctional Peptide Catalysis for Asymmetric Baeyer–Villiger Oxidations of Cyclobutanones. *ACS Catal.* **2019**, *9*, 242–252. (c) Mori, K.; Itakura, T.; Akiyama, T. Enantiodivergent Atroposelective Synthesis of Chiral Biaryls by Asymmetric Transfer Hydrogenation: Chiral Phosphoric Acid Catalyzed Dynamic Kinetic Resolution. *Angew. Chem., Int. Ed.* **2016**, *55*, 11642–11646.

(11) (a) Bürgi, T.; Baiker, A. Conformational Behavior of Cinchonidine in Different Solvents: A Combined NMR and ab Initio Investigation. *J. Am. Chem. Soc.* **1998**, *120*, 12920–12926. (b) Olsen, R. A.; Borchardt, D.; Mink, L.; Agarwal, A.; Mueller, L. J.; Zaera, F. Effect of Protonation on the Conformation of Cinchonidine. *J. Am. Chem. Soc.* **2006**, *128*, 15594–15595. (c) Maier, N. M.; Scheffzick, S.; Lombardo, G. M.; Feliz, M.; Rissanen, K.; Lindner, W.; Lipkowitz, K. B. Elucidation of the Chiral Recognition Mechanism of Cinchona Alkaloid Carbamate-type Receptors for 3,5-Dinitrobenzoyl Amino Acids. *J. Am. Chem. Soc.* **2002**, *124*, 8611–8629. (d) Prakash, G. K. S.; Wang, F.; Rahm, M.; Zhang, Z.; Ni, C.; Shen, J.; Olah, G. A. The Trifluoromethyl Group as a Conformational Stabilizer and Probe: Conformational Analysis of Cinchona Alkaloid Scaffolds. *J. Am. Chem. Soc.* **2014**, *136*, 10418–10431. (e) Hiemstra, H.; Wynberg, H. Addition of Aromatic Thiols to Conjugated Cycloalkenones, Catalyzed by Chiral. Beta-hydroxy Amines. A Mechanistic Study of Homogeneous Catalytic Asymmetric Synthesis. *J. Am. Chem. Soc.* **1981**, *103*, 417–430. (f) Li, H.; Liu, X.; Wu, F.; Tang, L.; Deng, L. Elucidation of the Active Conformation of Cinchona Alkaloid Catalyst and Chemical Mechanism of Alcoholysis of Meso Anhydrides. *Proc. Natl. Acad. Sci. U. S. A.* **2010**, *107*, 20625–20629. (g) Dijkstra, G. D. H.; Kellogg, R. M.; Wynberg, H.; Svendsen, J. S.; Marko, I.; Sharpless, K. B. Conformational Study of Cinchona Alkaloids. A Combined NMR, Molecular Mechanics and X-ray Approach. *J. Am. Chem. Soc.* **1989**, *111*, 8069–8076.

(12) For selected examples for enantioselectivity of reactions altered by population of cinchona alkaloids, see: (a) Aune, M.; Gogoll, A.; Mattsson, O. Solvent Dependence of Enantioselectivity for a Base-Catalyzed 1,3-Hydron Transfer Reaction. A Kinetic Isotope Effect and NMR Spectroscopic Study. *J. Org. Chem.* **1995**, *60*, 1356–1364. (b) Busygin, I.; Nieminen, V.; Taskinen, A.; Sinkkonen, J.; Toukonitty, E.; Sillanpää, R.; Murzin, D. Y.; Leino, R. A Combined NMR, DFT, and X-ray Investigation of Some Cinchona Alkaloid O-Ethers. *J. Org. Chem.* **2008**, *73*, 6559–6569.

- (13) Caner, H.; Biedermann, P. U.; Agrat, I. Conformational Spaces of (13) Cinchona Alkaloids. *Chirality* **2003**, *15*, 637–645.
- (14) (a) Yousefi, R.; Sarkar, A.; Ashtekar, K. D.; Whitehead, D. C.; Kakeshpour, T.; Holmes, D.; Reed, P.; Jackson, J. E.; Borhan, B. Mechanistic Insights into the Origin of Stereoselectivity in an Asymmetric Chlorolactonization Catalyzed by (DHQD)₂PHAL. *J. Am. Chem. Soc.* **2020**, *142*, 7179–7189. (b) Yousefi, R.; Ashtekar, K. D.; Whitehead, D. C.; Jackson, J. E.; Borhan, B. Dissecting the Stereocontrol Elements of a Catalytic Asymmetric Chlorolactonization: Syn Addition Obviates Bridging Chloronium. *J. Am. Chem. Soc.* **2013**, *135*, 14524–14527. (c) Ashtekar, K. D.; Vetticatt, M.; Yousefi, R.; Jackson, J. E.; Borhan, B. Nucleophile-Assisted Alkene Activation: Olefins Alone Are Often Incompetent. *J. Am. Chem. Soc.* **2016**, *138*, 8114–8119. (d) Marzijarani, N. S.; Yousefi, R.; Jaganathan, A.; Ashtekar, K. D.; Jackson, J. E.; Borhan, B. Absolute and Relative Facial Selectivities in Organocatalytic Asymmetric Chlorocyclization Reactions. *Chem. Sci.* **2018**, *9*, 2898–2908.
- (15) (a) Frisch, M. J.; Trucks, G. W.; Schlegel, H. B.; Scuseria, G. E.; Robb, M. A.; Cheeseman, J. R.; Scalmani, G.; Barone, V.; Petersson, G. A.; Nakatsuji, H.; Li, X.; Caricato, M.; Marenich, A.; Bloino, J.; Janesko, B. G.; Gomperts, R.; Mennucci, B.; Hratchian, H. P.; Ortiz, J. V.; Izmaylov, A. F.; Sonnenberg, J. L.; Williams-Young, D.; Ding, F.; Lipparini, F.; Egidi, F.; Goings, J.; Peng, B.; Petrone, A.; Henderson, T.; Ranasinghe, D.; Zakrzewski, V. G.; Gao, J.; Rega, N.; Zheng, G.; Liang, W.; Hada, M.; Ehara, M.; Toyota, K.; Fukuda, R.; Hasegawa, J.; Ishida, M.; Nakajima, T.; Honda, Y.; Kitao, O.; Nakai, H.; Vreven, T.; Throssell, K.; Montgomery, J. A., Jr.; Peralta, J. E.; Ogliaro, F.; Bearpark, M.; Heyd, J. J.; Brothers, E.; Kudin, K. N.; Staroverov, V. N.; Keith, T.; Kobayashi, R.; Normand, J.; Raghavachari, K.; Rendell, A.; Burant, J. C.; Iyengar, S. S.; Tomasi, J.; Cossi, M.; Millam, J. M.; Klene, M.; Adamo, C.; Cammi, R.; Ochterski, J. W.; Martin, R. L.; Morokuma, K.; Farkas, O.; Foresman, J. B.; Fox, D. J. *Gaussian 09*, Revision D. 01; Gaussian Inc.: Wallingford, CT, 2009. (b) Zhao, Y.; Truhlar, D. G. The M06 suite of density functionals for main group thermochemistry, thermochemical kinetics, noncovalent interactions, excited states, and transition elements: two new functionals and systematic testing of four M06-class functionals and 12 other functionals. *Theor. Chem. Acc.* **2008**, *120*, 215–241. (c) Grimme, S.; Ehrlich, S.; Goerigk, L. Effect of the damping function in dispersion corrected density functional theory. *J. Comput. Chem.* **2011**, *32*, 1456–1465.
- (16) Marenich, A. V.; Cramer, C. J.; Truhlar, D. G. Universal solvation model based on solute electron density and on a continuum model of the solvent defined by the bulk dielectric constant and atomic surface tensions. *J. Phys. Chem. B* **2009**, *113*, 6378–6396.
- (17) Glendening, E. D.; Badenhoop, J. K.; Reed, A. E.; Carpenter, J. E.; Bohmann, J. A.; Morales, C. M.; Karafiloglou, P.; Landis, C. R.; Weinhold, F. *NBO 7.0*; Theoretical Chemistry Institute, University of Wisconsin: Madison, WI, 2018. https://nbo7.chem.wisc.edu/biblio_css.htm (accessed 2021–07–01).
- (18) Bader, R. F. W. In *Atoms in Molecules: A Quantum Theory*; Clarendon Press: Oxford, 1990.
- (19) (a) Johnston, R. C.; Cheong, P. H.-Y. C–H...O non-classical hydrogen bonding in the stereomechanics of organic transformations: theory and recognition. *Org. Biomol. Chem.* **2013**, *11*, 5057–5064. (b) Berg, L.; Mishra, B. K.; Andersson, C. D.; Ekström, F.; Linusson, A. The Nature of Activated Non-classical Hydrogen Bonds: A Case Study on Acetylcholinesterase–Ligand Complexes. *Chem. - Eur. J.* **2016**, *22*, 2672–2681. (c) Molina, P.; Zapata, F.; Caballero, A. Anion Recognition Strategies Based on Combined Noncovalent Interactions. *Chem. Rev.* **2017**, *117*, 9907–9972.
- (20) Bader, R. F. W. A Bond Path: A Universal Indicator of Bonded Interactions. *J. Phys. Chem. A* **1998**, *102*, 7314–7323.
- (21) (a) Nishio, M.; Umezawa, Y.; Fantini, J.; Weiss, M. S.; Chakrabarti, P. CH- π Hydrogen Bonds in Biological Macromolecules. *Phys. Chem. Chem. Phys.* **2014**, *16*, 12648–12683. (b) Neel, A. J.; Hilton, M. J.; Sigman, M. S.; Toste, F. D. Exploiting Non-Covalent π Interactions for Catalyst Design. *Nature* **2017**, *543*, 637–646.
- (22) For a recent example of enantioselectivity affected by a remote bulky substituent on catalyst in asymmetric halogenation, see: Lu, Y.; Nakatsuji, H.; Okumura, Y.; Yao, L.; Ishihara, K. Enantioselective Halo-oxy- and Halo-azacyclizations Induced by Chiral Amidophosphate Catalysts and Halo-Lewis Acids. *J. Am. Chem. Soc.* **2018**, *140*, 6039–6043.
- (23) Hansch, C.; Leo, A.; Taft, R. W. A Survey of Hammett Substituent Constants and Resonance and Field Parameters. *Chem. Rev.* **1991**, *91*, 165–195.
- (24) For selected examples for correlation between enantioselectivity and substituents on catalyst/ligand, see: (a) Palucki, M.; Finney, N. S.; Pospisil, P. J.; Güler, M. L.; Ishida, T.; Jacobsen, E. N. The Mechanistic Basis for Electronic Effects on Enantioselectivity in the (salen)Mn(III)-Catalyzed Epoxidation Reaction. *J. Am. Chem. Soc.* **1998**, *120*, 948–954. (b) Jensen, K. H.; Sigman, M. S. Systematically Probing the Effect of Catalyst Acidity in a Hydrogen-Bond-Catalyzed Enantioselective Reaction. *Angew. Chem., Int. Ed.* **2007**, *46*, 4748–4750. (c) Yang, C.; Zhang, E.-G.; Li, X.; Cheng, J.-P. Asymmetric Conjugate Addition of Benzofuran-2-ones to Alkyl 2-Phthalimidoacrylates: Modeling Structure–Stereoselectivity Relationships with Steric and Electronic Parameters. *Angew. Chem., Int. Ed.* **2016**, *55*, 6506–6510.